THE JOURNAL OF PHYSICAL CHEMISTRY C

Article

pubs.acs.org/JPCC

New Insight into the Interface Chemistry and Stability of Glutathione Self-Assembled Monolayers on Au(111)

Flavia Lobo Maza,[†] Lucila Méndez De Leo,[‡] Aldo A. Rubert,[†] Pilar Carro,[§] Roberto C. Salvarezza,[†] and Carolina Vericat*[,†]

[†]Instituto de Investigaciones Fisicoquímicas Teóricas y Aplicadas (INIFTA), Facultad de Ciencias Exactas, Universidad Nacional de La Plata - CONICET Sucursal 4, Casilla de Correo 16, 1900 La Plata, Argentina

[‡]DQIAyQF, INQUIMAE-CONICET, Facultad Ciencias Exactas y Naturales, Universidad de Buenos Aires, Pabellón 2, Ciudad Universitaria, Buenos Aires C1428EHA, Argentina

[§]Área de Química Física, Departamento de Química, Facultad de Ciencias, Universidad de La Laguna, Instituto de Materiales y Nanotecnología, Avenida Francisco Sánchez, s/n, 38071, La Laguna, Tenerife, Spain

Supporting Information

ABSTRACT: In this paper we have studied glutathione (GSH) self-assembled monolayers (SAMs) on Au(111) prepared by incubation from solutions in phosphate buffer (pH = 7). These SAMs degrade with increasing immersion time to yield adsorbed S and polysulfide species on the gold surface, as revealed by cyclic voltammetry and X-ray photoelectron spectroscopy. Results from polarization modulation infrared reflection−absorption spectroscopy (PM-IRRAS) show that even if GSH decomposes on the surface the vibrational bands characteristic of the molecule are still present. This has direct relevance for the study of gold nanoparticles (AuNPs) protected by hydrophilic thiols and also for biomedical applications of GSH-capped AuNPs. Thiol exchange experiments of the drug 6-mercaptopurine (6MP) SAMs on Au(111) in contact with GSH solutions were also performed to better understand the possible role of the latter in the triggered release of 6MP from the surface of AuNPs for drug delivery applications. Our results show that 6MP is completely released only when a S adlayer, produced by desulfurization of GSH, is formed on the Au(111) surface.

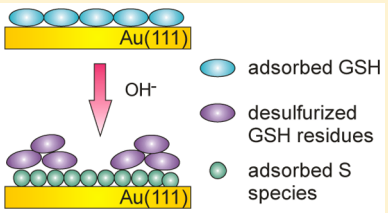

INTRODUCTION

Since their discovery in the 1980s, thiol self-assembled monolayers (SAMs) on metals, especially gold, have attracted the interest of both the surface science and nanotechnology communities.[1,2] Thiol SAMs on gold are robust and easy to prepare and represent fundamental building blocks for creating complex structures for nanotechnological applications that include sensors and biorecognition devices, drug-delivery systems, molecular electronics, and coatings for corrosion protection and tribological applications, among others.[1] These molecular monolayers have been used to link inorganic, organic, and biological materials to metallic planar surfaces and are widely used as capping agents in the synthesis of monodisperse metal nanostructures, which find applications in medicine, catalysis, photonics, and electronics.[1,3]

Even if thiol SAMs on gold, and especially thiol-capped gold nanoparticles (AuNPs), are extensively used in nanomedical and other nanotechnological applications, several aspects such as the real structure and the chemical nature of the interface, or the stability of the SAMs in physiological media are at best subject to intense debate in the scientific community, or sometimes simply neglected. The study of thiol SAMs on the Au(111) surface is especially relevant, as this is the lowest energy surface, and AuNPs are mostly formed by {111} planes.[4]

Alkanethiol SAMs on Au(111), particularly, have been extensively studied by many groups by using every possible surface characterization technique and have become a model system in surface science.[2] In spite of this, the true nature of the interface is still a matter of discussion regarding the reconstruction of the (111) surface with the formation of gold−thiolate complexes.[5−9]

More complex thiols, like those with hydrophilic terminal groups, have been much less studied and in some cases have been observed to undergo desulfurization to yield S adlayers on the gold surface. This is the case, for example, of some thiols with carboxylic acid groups in the α position with respect to the C−S bond, as thioacetic and thiomalic acids.[10,11] This point is especially interesting because some of these thiols are usual capping molecules in gold nanoparticles and nanoclusters for different nanotechnological applications (especially biomedical), as they can be straightforwardly employed to bind proteins and other biomolecules.

Glutathione (GSH) is a tripeptide formed by glutamic acid (Glu), cysteine (Cys) and glycine (Gly) and is the most important nonprotein thiol in the cell. Its intracellular concentration is 0.5−10 mM, while extracellular values are 1−3 orders of magnitude lower.[12] GSH is the most relevant cellular antioxidant, as it acts as an efficient scavenger for

Received: December 27, 2015
Revised: May 23, 2016
Published: May 25, 2016

DOI: 10.1021/acs.jpcc.5b12643
J. Phys. Chem. C 2016, 120, 14597−14607

reactive oxygen species such as free radicals and peroxides.[13] Also, glutathione reduces disulfide bonds formed within cytoplasmic proteins to cysteines by acting as an electron donor, and in turn is converted to its oxidized form, glutathione disulfide (GSSG).[14] Because of its high concentration in cells, GSH has been proposed as a good candidate to induce the release of other thiol-bearing biomolecules from the surface of the nanoparticle by the ligand exchange method,[15,16] a strategy of interest for drug delivery applications.[17−20] Moreover, GSH has been recently used as capping agent in gold nanoclusters for use as radiosensitizers in cancer radiotherapy.[21] In addition to its role as a ligand, it has been reported that GSH acts as an effective etchant in the synthesis of noble metal nanoclusters.[22,23]

In spite of the importance of GSH in biological systems and the promising use of GSH-capped gold nanostructures for nanobio applications, GSH SAMs on gold, and in particular on the Au(111) surface, have not been extensively studied. Some works have explored the property of GSH SAMs of acting as an "ion gate" with different charged species.[24−26] Also, several studies involving vibrational spectroscopy have contributed to the understanding of the GSH self-assembly kinetics from ethanolic solutions[27] and the molecule structural changes produced by changes in pH.[28−31] In some cases, these vibrational studies have been complemented by photoelectron spectroscopy measurements.[31]

In this paper we have studied GSH SAMs on Au(111) prepared by incubation from solutions in phosphate buffer (pH = 7). Interestingly, we have found that these SAMs degrade with increasing immersion time to yield S and polysulfide species adsorbed on the gold surface, a result that has direct relevance in the use of GSH-capped AuNPs for biomedical applications. Also, the role of GSH (and sulfide) in thiol exchange experiments on Au(111) surface was studied by using 6-mercaptopurine (6MP), a synthetic thiol employed in the treatment of some types of leukemia and autoimmune diseases. This drug has been previously immobilized on AuNPs in order to improve its administration[32] and, once inside the cell, needs to be released from the gold surface of the nanoparticle, a process that can be triggered by GSH, as proposed by Rotello et al.[17] Our results on Au(111) show that complete release of 6MP takes place only for times longer than 24 h and that in those conditions it is a S adlayer that is formed on the gold surface rather than a GSH SAM.

MATERIALS AND METHODS

Experimental Procedure. L-Glutathione reduced (GSH) (Sigma-Aldrich, ≥ 98%), 6-mercaptopurine monohydrate (6MP) (Aldrich, 98%), NaOH (Emsure, Merck, ≥ 99%), Na_2HPO_4 (Baker, PA), NaH_2PO_4 (Baker, PA), anhydrous Na_2S (Aldrich), and absolute ethanol (Carlo Erba, 99.5%) were used as received. Ultrapure water (Millipore Products, Bedford) was used to prepare all solutions and for rinsing. Evaporated Au films on glass with (111) preferred orientation (AF 45 Berliner Glass KG, Germany) were used as substrates. After annealing for several minutes with a hydrogen flame, these Au substrates exhibit atomically smooth (111) terraces (300−500 nm wide) separated by steps of monatomic height, as revealed by scanning tunneling microscopy (STM). Henceforth, we shall refer to the annealed gold substrates as Au(111).

Glutathione SAMs on Au(111) were prepared by immersion of the clean substrates in freshly prepared 5 mM GSH solutions in 10 mM phosphate buffer (pH = 7). Different incubation times (t_{SAM}) were used, typically between 1 and 48 h (in some cases t_{SAM} = 10 min was employed). After SAM formation samples were removed from the solution, rinsed with ultrapure water, dried with N_2, and either immediately placed in an electrochemical cell for cyclic voltammetry (CV) measurements, analyzed by PM-IRRAS (polarization modulation infrared reflection adsorption spectroscopy) or XPS (X-ray photoelectron spectroscopy), or imaged in air by STM (see Supporting Information). In some cases, 1-week old GSH solutions were used for CV experiments. Moreover, SAMs prepared either from 5 mM solutions in water (pH = 3.5; see Supporting Information) or 0.1 M NaOH (pH = 13; data not shown) were prepared for comparative CV experiments. Sulfur SAMs on Au(111) were prepared by incubation of the clean substrates in 1−5 mM Na_2S solutions in 10 mM phosphate buffer (pH = 7) for 1 h.

Thiol Exchange Experiments. 6MP SAMs on Au(111) were prepared by immersion in 100 μM ethanolic solutions for 24 h. The substrates were rinsed with ethanol and dried and then immersed in GSH solution for 1, 24, or 48 h. Samples were rinsed with water, dried with N_2, and either placed in the electrochemical cell for CV or in the sample holder for PM-IRRAS measurements.

Electrochemical Measurements. Cyclic voltammetry was performed with a potentiostat with digital data acquisition (TEQ, Argentina). The thiol-modified Au(111) substrate (working electrode) was mounted in a conventional three-electrode glass cell with a Pt large area wire as counter and a saturated calomel electrode (SCE) as reference electrodes, respectively. Aqueous 0.1 M NaOH solutions were degassed with purified nitrogen prior to the experiments.

Thiol reductive electrodesorption was performed by scanning the potential from −0.2 to −1.4 at 0.05 V s^{-1} in the 0.1 M NaOH solution at room temperature. The charge density involved in the reductive desorption was calculated by integrating the peak area and taking into account the electrode real area from the gold oxide reduction peak corresponding to the process $AuO + 2e^- + H_2O \rightarrow Au + OH^-$. The surface coverage of the SAM was calculated from the charge density, considering 440 μC cm^{-2} for a gold oxide monolayer on the Au(111) surface.

X-ray Photoelectron Spectroscopy Measurements. An Al Kα source at 1486.6 eV (XR50, Specs GmbH) and a hemispherical electron energy analyzer (PHOIBOS 100, Specs GmbH) operating either at 10 or 40 eV pass energy were used in the measurements. A two-point calibration of the energy scale was performed using sputtered cleaned gold (Au $4f_{7/2}$, binding energy =84.00 eV) and copper (Cu $2p_{3/2}$, binding energy = 932.67 eV) samples. C 1s at 285 eV was used as charging reference. Spectra were analyzed with CasaXPS v2.3.14 and XPS Peak 4.1 software packages. Shirley-type backgrounds were used in the fitting procedure of high resolution spectra. For quantitative analysis, peak intensities were corrected by the corresponding relative sensitivity factors (RSF).

The fitting of the S 2p peaks was carried out by using a spin−orbit splitting of 1.19 eV and a branching ratio of 0.5. The main criterion for adding extra components in the present S 2p spectra was based on comparison with well-established fwhm values and G-L ratios of the peaks determined from the measurement (in the exactly same experimental conditions) of a large number of SAMs on Au(111) prepared from thiols that do not suffer significant degradation in contact with the gold

DOI: 10.1021/acs.jpcc.5b12643
J. Phys. Chem. C 2016, 120, 14597−14607

surface (like alkanethiols or 6-mercaptopurine) and with optimized rinsing procedures, together with stoichiometric analyses and the correlation with blank samples of relevance for this system.

Polarization Modulation Infrared Reflection Adsorption Spectroscopy Measurements. PM-IRRAS experiments were performed on a Thermo Nicolet 8700 (Nicolet) spectrometer equipped with a custom-made external table-top optical mount, a MCT-A detector (Nicolet), a photoelastic modulator (PEM; PM-90 with II/Zs50 ZnSe 50 kHz optical head, Hinds Instrument), and synchronous sampling demodulator (GWC Instruments). The IR spectra were acquired with the PEM set for a half wave retardation at 1600 cm^{-1}. The angle of incidence was set at 80°, which gives the maximum of mean square electric field strength for the air/gold interface. The demodulation technique developed by Corn was used in this work.[33,34] The signal was corrected by the PEM response using a method described by Frey et al.[35] 1500 scans were performed, and the resolution was set for 4 cm^{-1}.

Density Functional Theory Calculations. Density functional calculations have been performed with the periodic plane-wave basis set code VASP 5.2.12.[36,37] We have followed the scheme of nonlocal functional proposed by Dion et al.,[38] vdW-DF, and the optimized Becke88 exchange functional optB88-vdW[39] to take into account van der Waals (vdW) interactions. The electronic wave functions were expanded in a plane-wave basis set with a 450 eV cutoff energy. The projector augmented plane wave (PAW) method has been used to represent the atomic cores with PBE potential.[40] Gold surfaces were represented by a five atomic layer slab with ∼18 Å vacuum. Optimal grid of Monkhorst−Pack[41] k-points of 3 × 9 × 1 has been used for numerical integration in the reciprocal space of the $(3\sqrt{3} \times \sqrt{3})R30°$ surface structure. Surface relaxation is allowed in the three uppermost Au layers of the slab. GS radical species were optimized in an asymmetric box of 30 Å × 28 Å × 29 Å.

The average binding energy per adsorbed GS* radical, which results when GSH loses the hydrogen atom of the S−H group on Au(111) surface, E_b, is defined in eq 1:

$$E_b = [E_{GS*/Au} - E_{Au(111)} - E_{GS*}] \quad (1)$$

where, $E_{GS*/Au}$, $E_{Au(111)}$ and E_{GS*} stand for the total energy of the adsorbate−substrate system, the Au slab, and the GS* radical, respectively. A negative number indicates that adsorption is exothermic with respect to the separate clean surface and GS* radical.

RESULTS AND DISCUSSION

GSH SAMs on Au(111). Glutathione (GSH) is a tripeptide formed by amino acids glutamate (Glu), cysteine (Cys) and glycine (Gly) which has an unusual γ-peptide bond between Glu and Cys to prevent GSH from being hydrolyzed by most peptidases. GSH presents four acid dissociation equilibria with the following pK_a values: pK_1 = 2.12 (−COOH of Glu); pK_2 = 3.59 (−COOH of Gly); pK_3 = 8.75 ($-NH_3^+$); pK_4 = 9.65 (−SH).[42] Thus, different GSH species (cationic, zwitterionic and several anionic forms) can be found at different pH values. Scheme 1a shows the structure of the anionic form of GSH that predominates in solution at pH = 7 (almost 100%, from the GSH species distribution diagram).

Figure 1 shows typical cyclic voltammograms (0.05 V s^{-1} in 0.1 M NaOH solution) of GSH SAMs prepared by incubating the gold substrates in 5 mM glutathione solutions in phosphate

Scheme 1. (a) Anionic Glutathione (GSH); (b) 6-Mercaptopurine (6MP)

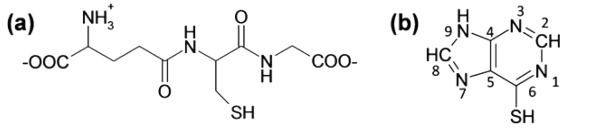

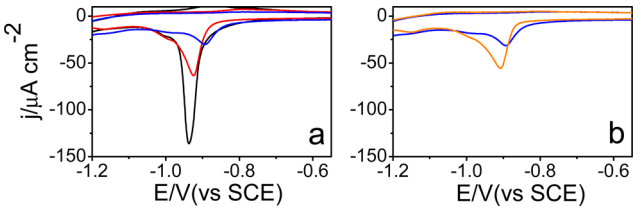

Figure 1. Cyclic voltammograms of Au(111) samples prepared by immersion in 5 mM GSH solution in 10 mM PB (pH = 7). (a) Samples prepared with different incubation times: 1 h (blue), 24 h (red), and 48 h (black). (b) Sample incubated for 1 h and further immersed in PB for 23 h (orange). The CV corresponding to 1 h incubation has been included for comparison (blue). Scan rate: 0.05 V s^{-1}. Electrolyte: 0.1 M NaOH.

buffer (PB) 10 mM (pH = 7) for different incubation times (t_{SAM}). Even if GSH molecules in aqueous solutions readily oxidize in air to give GSSG species, disulfide adsorption on the Au(111) surface is expected to yield thiol SAMs similar to those formed from thiol solutions.[2] In all the current/potential profiles there is a cathodic peak that, in principle, can be attributed to the well-known reductive desorption of the thiol SAM according to reaction RS-Au(111) + e^- → RS^- + Au(111).[43] The absence of anodic peaks in the positive scan indicates that no significant readsorption of the desorbed species takes place, a fact that is consistent with the high solubility of the reaction products in aqueous solutions.

For t_{SAM} = 1 h (blue trace in Figure 1a), the peak appears at potential E = −0.88 V ± 0.02 V. The calculated charge density (Q) value for the reduction peak is 30 ± 5 μC cm^{-2}, which corresponds to a thiol surface coverage θ = 0.13. This coverage is already attained for t_{SAM} = 10 min and can be assigned to a complete GSH SAM, taking into account the size of this molecule (the projected surface area of adsorbed glutathione, from DFT calculations, is ≈35 $Å^2$). For larger incubation times, there is a slight shift of the electrodesorption peak to more negative potentials and, more important, a significant increase in the peak charge that now is inconsistent with a GSH SAM due to steric reasons. In fact, for t_{SAM} = 24 h (Figure 1a, red line) and t_{SAM} = 48 h (Figure 1a, black line), E = −0.93 V ± 0.02 V, while Q values are 91 ± 15 μC cm^{-2} and 140 ± 10 μC cm^{-2}, respectively. Similar results were obtained with GSH solutions at pH = 7 in the absence of phosphates, i.e., prepared by adjusting the initial pH in water (≈ 3.5) with a concentrated NaOH solution. Also, the same trend is found for GSH SAMs prepared by incubation from 5 mM solutions in 0.1 M NaOH (pH = 13), although in this case higher Q values are obtained for shorter times compared to pH = 7. By contrast, in the case of SAMs prepared by incubation in 5 mM GSH aqueous solutions (pH = 3.5), Q values do not show marked differences from those obtained for t_{SAM} = 1 h in pH = 7 solutions, although a slight increase in charge density is observed with increasing t_{SAM} (see Figure S1 in the Supporting Information).

The important increase in Q, incompatible with a GSH SAM, that is observed for long incubation times in the GSH solutions

DOI: 10.1021/acs.jpcc.5b12643
J. Phys. Chem. C 2016, 120, 14597−14607

at pH = 7 (and higher) lead us to believe that some kind of degradation of the GSH SAM takes place that involves the formation of small sulfur species on the Au(111) surface. It is well-known that monomeric S is reduced in a two-electron process upon electrodesorption according to S−Au(111) + $2e^-$ → S^{2-} + Au(111) at potential values similar to those observed in our voltammograms.[44] At first one could think that decomposition of GSH/GSSG can occur in solution. Indeed, complex enzyme-mediated decompositions occur in the cell[45] and also nonenzymatic degradation mechanisms for neutral GSH solutions that involve disulfide formation have been proposed from NMR data.[46] However, we have obtained similar results as in Figure 1 for t_{SAM} = 1 h (Q ≈3 0 μC cm^{-2}) for samples incubated for 1 h in GSH solutions at pH = 7 that were aged for 1 week prior to incubation, a time period greater than the largest t_{SAM} studied in this work. Moreover, it should be mentioned that, even for GSH SAMs incubated for t_{SAM} = 48 h, Q values are significantly lower than for samples prepared by incubation in sulfide solutions (300−500 μC cm^{-2} vs ≈ 140 μC cm^{-2}) (see Figure S2a in the Supporting Information). Therefore, we can conclude that GSH/GSSG in solution (pH = 7) is not significantly decomposed to sulfide species (H_2S, HS^-) in the time lapse of our experiments.

It is thus reasonable to assume that the Au(111) surface has a role in the GSH degradation. In order to assess this point we have prepared GSH SAMs on Au(111) (t_{SAM} = 1 h) and further immersed them for 23 h in GSH-free phosphate buffer solution (pH = 7). The corresponding CV in 0.1 M NaOH is shown in Figure 1b (orange line): the peak potential shifts to −0.91 V and Q increases to 72 ± 7 μC cm^{-2}, i.e., approximately twice the value for a GSH SAM with t_{SAM} = 1 h (blue line). Thus, GSH molecules adsorbed on Au(111) degrade with time to yield a S submonolayer, showing that the metal surface has a key role in the degradation process.

Representative high resolution XPS spectra are shown in Figure 2 for GSH SAMs on Au(111) incubated for t_{SAM} = (a) 1 h and (b) 48 h. In both cases, three components were needed to adequately fit the S 2p region: S1 (≈161 eV), S2 (≈162 eV), and S3 (163−164 eV), as already reported by several authors.[2,47−49] S2 is main component in the spectra and in principle can be assigned to chemisorbed thiolate on gold, as in the case of alkanethiols on Au(111).[50] Two additional minor components may be present in thiol SAMs on Au(111): one at ≈161 eV, which has been attributed either to the presence of monomeric sulfur (arising from thiol degradation or from sulfide impurities in the thiol reagent) or to thiol adsorption on multiple sites,[51] and another one at ≈163 eV that has been assigned both to unbounded thiol molecules and to disulfides. Most SAMs of alkanethiol on Au(111) only present the S2 component when properly rinsed to remove unbounded molecules. While the signal-to-noise ratio in the spectra is lower than for other thiol SAMs due to the low coverage (θ = 0.13 for GSH vs θ = 0.33 for a typical alkanethiol), we did not increase acquisition time to avoid damage of the SAM induced by radiation, which can result either in the increase of S3[52] or S1 components.[49]

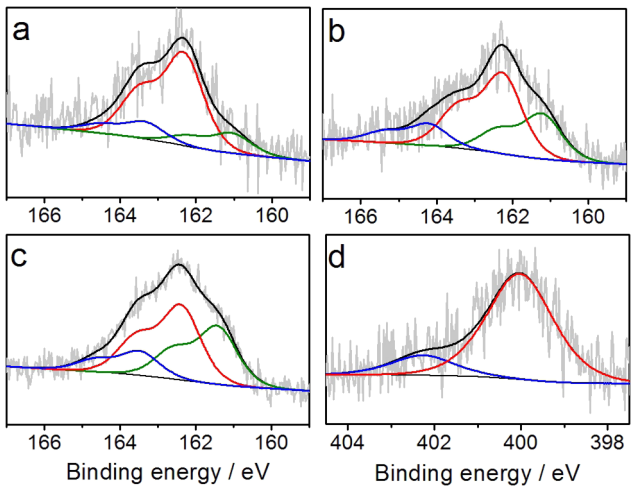

Figure 2. High-resolution XP spectra: (a) and (b) S 2p region of Au(111) samples immersed for (a) t_{SAM} = 1 h and (b) t_{SAM} = 48 h in GSH 5 mM solution at pH = 7; (c) S 2p region of a S monolayer on Au(111) prepared from a Na_2S solution (pH = 7); (d) typical N 1s region of a Au(111) sample prepared by immersion in GSH 5 mM solution at pH = 7 (t_{SAM} = 1 h)). Spectra a−c have been fitted with three components: S1 (green), S2 (red) and S3 (blue), while that in panel d shows two distinct types of N (traces in red and blue) (see the text for details).

A more accurate assignment of the S 2p XPS components in Figure 2 can be made if we take into account results from cyclic voltammetry, which indicate that S species are formed upon GSH adsorption with increasing t_{SAM}. Based on blank measurements for S SAMs on Au(111) at pH = 7 (Figure 2c) and on the assignment made in previous works for S SAMs prepared from alkaline solutions,[53,54] the component at ≈162 eV can be assigned to adsorbed polymeric S species and that at ≈161 eV to monomeric S, while a third minor component, which is not always present and whose position is more variable (163−164 eV), can be attributed to S species weakly bounded to the gold surface (elemental S and polysulfide multilayers).

As expected from CV results, S 2p/Au 4f intensity ratios are highest for SAMs incubated for 48 h, followed by t_{SAM} = 24 h and then 1 h. However, in neither case the values reach those of S layers on Au(111). For t_{SAM} = 48 h there is a clear increase in the proportion of the 161 eV component, noticeable even without peak fitting, an indication that more S species are present in the interface. Thus, it can be concluded that for the spectra in Figure 2a,b, the main component (S2) arises from two different contributions: chemisorbed GSH (as thiolate) and some adsorbed polymeric S species, the latter increasing with increasing t_{SAM}. Component S3 (≈ 10% of the total peak area for all t_{SAM} values) can be assigned to the presence of some unbounded GSH molecules or disulfides (GSSG) and also to a certain amount of elemental S, while component S1 can be attributed mainly to monomeric S. The small amount of component S1 present in the spectra of 1 h incubation SAMs that is detected by XPS (<10%) is not clearly revealed by CV but indicates that some degradation already occurs at short times. Moreover, for all incubation times, spectra do not show any S 2p signals at BE > 166 eV, i.e., no oxidized S species (like sulfonates) are present on the Au surface.

It should be mentioned that there are some previous XPS studies of the S 2p region of GSH SAMs, prepared by incubation in aqueous solutions at different pH values whose spectra have been fitted with a single doublet at ≈162 eV (S2 component).[29,55] In contrast, for GSH samples on Au(111) prepared by vapor dosing in UHV, a second component at ≈163 eV (S3) was included which was attributed to unbounded GSH molecules.[31] Regarding the absence of the S1 component in previous works, in ref 29 even if incubation times for SAM preparation were 20 min, significantly lower than those used in

DOI: 10.1021/acs.jpcc.5b12643
J. Phys. Chem. C 2016, 120, 14597−14607

these work, some increase in the peak intensity at BE ≈161 eV can be observed with increasing pH, while in ref 55 the shape of the spectrum (corresponding to a GSH SAM prepared by 24 h incubation in aqueous GSH solution) is compatible with an additional doublet at ≈161 eV.

On the other hand, for the different incubation times (1, 24, and 48 h), the N 1s region can be adequately fitted with two components (see Figure 2d for t_{SAM} = 1 h): the most intense one (N1), at 400−401 eV, can be assigned both to nonprotonated primary amines and amides (red line), while N2 (BE 401−402 eV) corresponds to protonated primary amines (blue line).[29] Ideally, at pH = 7 the N1/N2 intensity ratio for GSH should be equal to 2, as there are two amide bonds and the primary amine is fully protonated (see Scheme 1). However, in all cases, the experimental ratio is higher than 2, a fact that would imply that some primary amines are actually deprotonated.

A more relevant fact is that a significant N 1s signal is present even for samples incubated for 24 or 48 h. Even more, in all cases the N 1s/S 2p peak intensity ratio is close to 3, as expected from the stoichiometry of GSH. This reveals that for such incubation times the resulting interface is not only composed of the S species produced by the desulfurization of GSH but also of the residues of this reaction and a small amount of intact (i.e., nondegraded) molecules that are probably in a physisorbed state (S3 is always a minor component).

To further characterize glutathione SAMs on Au(111) at pH = 7, especially regarding its decomposition on the surface, we have performed PM-IRRAS measurements of GSH SAMs on Au(111) corresponding to t_{SAM} = 1, 24, and 48 h. The different spectra (Figure 3) show several characteristic bands that are

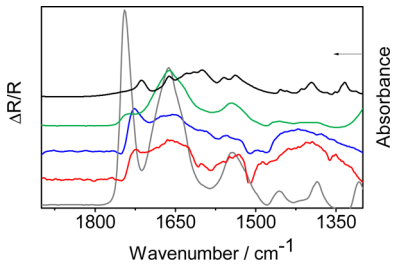

Figure 3. Vibrational IR spectra of GSH. Black line: FTIR transmission spectrum of GSH in a KBr pellet. PM-IRRA spectra of Au(111) samples prepared by incubation in 5 mM GSH solutions in phosphate buffer (pH = 7) for different t_{SAM}: 1 h (blue), 24 h (red) and 48 h (gray). The spectrum in green corresponds to a S SAM on Au(111) subsequently exposed for 24 h to a GSH solution. The intensity of the spectra in black and gray have been divided by a factor of 10, and that in green by a factor of 5.

consistent with those reported in the literature[28,29] and with the transmission spectrum of GSH in KBr (black line in Figure 3). The position of the absorption peaks found for GSH SAMs on Au(111) and their assignment based on the literature are summarized in Table 1. It is worth mentioning that in all cases no peaks characteristic of S, organic disulfides, or polysulfide species are expected within the available wavelength range.

For t_{SAM} = 1 h, the spectra (blue line in Figure 3) show a strong band at 1724 cm^{-1} that has been assigned to the symmetric stretching of C═O in protonated carboxylic acid groups that are probably involved in hydrogen bonds but not dimerized.[56] There is also a band at ∼1660 cm^{-1} that

Table 1. Assignments for PM-IRRA Spectra of GSH and 6MP SAMs on Au(111)[a]

GSH		6MP	
ν (cm^{-1})	assignment[28]	ν (cm^{-1})	assignment[62]
≈1730	ν_S(C═O) in COOH	1593−1572	δ_{ip}N1−H+νC5−N7+ δ_{ip}R5,R6
1674	amide I: ν_S (C═O) in amide	1465	δ_{ip}C8−H+δ_{ip}N1−H+ δ_{ip}R5,R6+νC8−N7
1599	ν_S (COO^-)	1409−1399	δ_{ip}R5,R6
1556	amide II: N−H bend and C−N stretch	1330	δ_{ip}C8−H+δ_{ip}C2−H+νC−N7−C8+δ_{ip}N9−H
1497	δ-CH_2		
1420−1376	ν_S (COO^-)		

[a] ν: wavenumber; δ: vibration; δ_{ip}: in plane vibration; ν_s: stretching vibration; R5: five-member ring; R6: six- member ring. *See the text for details.

corresponds to the symmetric stretching absorption of C═O in amides (amide I) and another one at 1556 cm^{-1} that has been assigned to amide II vibration and involves both C−N stretch and C−N−H in-plane bend in the stretch bend mode.[28,57] Moreover, two bands at 1599 and 1420 cm^{-1} have been assigned to COO^- stretching, and are indicative of the presence of ionized acid moieties.

The reason why there are bands from both ionized and protonated carboxylic groups in the PM-IRRAS spectra, even if at pH = 7 both carboxylates should be deprotonated (considering the pK_a values of GSH), could be due to the fact that the pK_a values of COOH (and NH_3^+) of adsorbed GSH on Au(111) are probably different from the values for GSH in aqueous solution. For instance, in the case of simpler ω-carboxy and ω-amine n-alkanethiols, the pK_a values of COOH- (NH_2-) terminated SAMs can be 2−4 pH units higher (lower) than the corresponding thiol in aqueous solution.[58,59] This effect would not only explain the presence of a band typical of protonated carboxylic acid groups in our spectra, which can shift to lower wavenumbers upon hydrogen bond formation,[60] and which would correspond to the COOH of Gly, but also the obtained XPS N1/N2 intensity ratios, which show a higher proportion of amines in a deprotonated state than expected from the pK_a values of GSH in solution. Moreover, local pH changes as a result of water rinsing and drying of the SAM,[61] which are necessary steps for PM-IRRAS and XPS measurements, can contribute to the presence of the observed COOH stretching band.

Spectra corresponding to t_{SAM} = 24 h (red line in Figure 3) are comparable to those for 1 h: the bands appear at the same wavenumbers and have similar intensities. However, spectra corresponding to t_{SAM} = 48 h (gray line in Figure 4) are notably different to the other two: the same bands are present but better resolved and with much higher intensities. Interestingly, the band assigned to symmetric stretching of C═O in protonated carboxylic acid groups shifts to higher wavenumbers (1742 cm^{-1} vs 1724 cm^{-1}), and this would imply that in this case there is not a significant amount of H bonds.

It is worth mentioning that, both for Au(111) samples immersed in GSH solution for t_{SAM} = 24 and 48 h, even if CV and S 2p XPS results show an important degradation of the

DOI: 10.1021/acs.jpcc.5b12643
J. Phys. Chem. C 2016, 120, 14597−14607

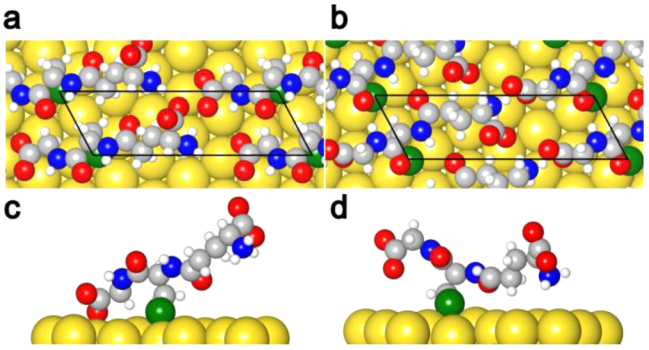

Figure 4. Top and side views of the optimized structures of the $(3\sqrt{3} \times \sqrt{3})R30°$ GS lattice on the unreconstructed Au(111) surface: (a and c) tilted and (b and d) upright configurations of anionic GSH. Color of the atoms: yellow, Au; green, S; gray, C; white, H; red, O atoms; blue, N.

GSH SAMs to yield adsorbed S/polysulfide species, the presence of characteristic bands of GSH in the PM-IRRA spectra and the N 1s/S 2p XPS peak intensity ratio indicate that some residues from desulfurization of GSH and also a small amount of intact (i.e., non degraded) GSH molecules remain in the interface, probably physisorbed on the S adlayer. This is supported by the fact that characteristic GSH bands also appear in spectra of samples consisting of S adlayers on Au(111) that are further immersed in GSH 5 mM solution for 24 h (green line in Figure 3). Also in this case, as for t_{SAM} = 48 h, the symmetric stretching of C═O in protonated carboxylic acid groups shifts to higher wavenumbers, probably indicating the absence of hydrogen bonds.

In summary, both IR spectra and the S/Au and N/S intensity ratios obtained from XPS data show that for t_{SAM} = 48 h there is a larger amount of residues, i.e., products of the decomposition of the molecule upon adsorption on the gold surface, probably in more than one layer, and also some GSH/GSSG molecules on the S adlayer, while for t_{SAM} = 24 h there is a smaller amount of GSH residues and GSH/GSSG molecules. Interestingly, this result shows that the presence of vibrational bands characteristic of GSH is not enough to conclude that this is adsorbed on the gold surface as an intact molecule, i.e., without degradation to some kind of S species, as the residues (which can give rise to the same characteristic bands) may remain physisorbed. This is particularly relevant for the case of gold nanoparticles capped with thiol ligands of biological importance (like GSH), which could be degraded to sulfide species and whose residues could remain adsorbed on the surface even after purification. Moreover, the ability of GSH to act as an etchant in the synthesis of small gold nanoparticles and nanoclusters (and also nanoclusters of other noble metals) could be related to the formation of sulfide species.[22,23]

As mentioned above, experimental results show that GSH on Au(111) at pH = 7 degrades with time to yield adsorbed monomeric and polymeric S, a process that becomes more evident with increasing pH. Even for t_{SAM} = 1 h, slight degradation takes place, as revealed from the photoelectron S 2p spectra and the broad desorption peaks. Because only those GSH molecules that are chemisorbed on the Au(111) surface (or in close contact to the metal) experience degradation, it can be stated that the Au(111) surface in some way promotes the rupture of C−S bonds to yield the S species. To the best of our knowledge, this is the first time that the desulfurization of GSH SAMs on Au(111) prepared at pH = 7 is reported.

There are several studies dealing with the decomposition of GSH, cysteine and S-bearing peptides and proteins, although generally in strong alkaline solutions and under boiling conditions.[46,63−65] Two main processes have been identified—desulfurization and peptide bond cleavage—both of which are favored by increasing solution pH.[66] Although the studies mostly agree on the fact that disulfides are formed as intermediates, there are some differences among them regarding the exact mechanism and the nature of the final products.[64,65,67] In the case of the desulfurization reaction, it has been concluded from NMR measurements that γ-glutamyldehydroalanylglycine molecules can be formed by alkali treatment of the oxidized formed of GSH (the disulfide, GSSG).[68,69] This is consistent with the fact that the most relevant IR bands (those corresponding to carboxylates, amides, etc.) are observed in all the spectra of our work, independent of the SAM preparation time.

As regards the decomposition of glutathione at neutral pH, in addition to the knowledge about enzymatic degradation processes of GSH and related species in cells,[45,70,71] there are only a few studies about nonenzymatic GSH degradation in neutral solutions, although there is agreement on the fact that it is much slower than in alkaline media.[46,66] Indeed, in ref 46 it was shown from NMR results for GSH solutions in PB pH = 7.4 at 37 °C that significant degradation occurs only after ≈30 days and involved Glu-Gly peptide bond breakage and the formation of sulfenic acid. In the present work, however, GSH solutions (which can contain GSSG species because reduced glutathione readily oxidizes with air) were freshly prepared in all cases and, in spite of this, desulfurization was already detected for t_{SAM} > 6 h (data not shown) and was completely evident for 24 and 48 h.

Therefore, the Au(111) surface in some way promotes the desulfurization reaction in mild conditions (pH = 7 and room temperature), and this process is favored with increasing pH. A similar behavior has been observed for mercaptopyridine on Au(111) incubated from aqueous alkaline solutions, and a mechanism involving disulfide formation on the surface was proposed whose final product was a complete S adlayer on the metal surface.[72] Taking into account the evidence from the literature, it is not unreasonable to think that the desulfurization process of adsorbed GSH on Au(111) also proceeds via a disulfide mechanism and that the strong adsorption of the sulfide species on the (111) surface is the driving force. It can be pointed out that, as adsorbed GSH degrades to yield a S diluted layer, more molecules can reach the gold surface and in turn desulfurize, thus explaining the S coverage. The fact that S coverage never reaches that found when adsorption takes place from sulfide solutions suggests that the GSH degradation process should involve adjacent molecules. Also, it is possible that the residues of desulfurization (probably γ-glutamyldehydroalanylglycine molecules) block the access of new GSH molecules to the Au(111) surface. In any case, a detailed study of the desulfurization reaction mechanism on Au(111) is clearly beyond the scope of the present work. Whatever the mechanism is, it remains to be studied whether GSH SAMs on the other low Miller index faces of Au present the same stability, especially on the Au(100) surface, as gold nanoparticles are formed mainly by {111} but also {100} facets.

DFT calculations have been performed to explore the energetic and structural characteristics of GSH SAM on Au(111). Data for 6MP SAM on Au(111) (Figure S5 in the Supporting Information) have been included and will be

DOI: 10.1021/acs.jpcc.5b12643
J. Phys. Chem. C 2016, 120, 14597−14607

addressed in the next section. As revealed from in air STM imaging (see Figure S3 in the Supporting Information), no long-range order is found for GSH SAMs on Au(111), in resemblance to what it has been already reported for 6MP on Au(111).[6] In spite of this, in order to make calculations and based on the CV for nondegraded SAMs (t_{SAM} = 1 h) which yield θ_{GSH} = 0.13, and also from XPS and STM imaging, a $(3\sqrt{3} \times \sqrt{3})$R30° unit cell with one molecule of GSH was proposed which has been modeled on an unreconstructed (111) surface (θ_{GSH} = 0.11). For clarity, in Figure 4c,d only the topmost gold layer has been depicted. We have considered the anionic form of GSH (Figure 4), and two different GS-Au configurations have been analyzed: one which only interacts with the Au(111) surface through the thiol group forming a covalent thiolate-Au bond, termed "upright" GSH, and another one that interacts with the surface not only through the S head (as the other one), but also through the negatively charged O atom of the carboxylate group of glycine, as already proposed by Bürgi et al.,[28] and which we have named "tilted" GSH.

Table 2 shows some energetic parameters of GS-Au for both anionic GSH configurations. Comparison of the surface free energies (γ) for the two configurations of GSH considered shows that, as expected, the interaction of the COO- of glycine with the Au surface yields a more stable structure. As reported for other thiols on Au, the analysis of Bader charges for the upright and tilted structures reveals that the Au(111) surface atoms have a positive charge of 0.05, while the S atoms exhibit negative charges −0.10 and −0.17, respectively. More interesting, for the tilted molecule the O atom interacting with the metal surface has a large negative charge (−1.63), while the closest Au atom has the highest positive charge (+0.16), suggesting that its better stabilization arises from an electrostatic interaction in addition to the covalent S−Au bonding.

Table 2. Energetic Parameters and Bader Charges for $(3\sqrt{3} \times \sqrt{3})$R30°-GS and $(3\sqrt{3} \times 2)$-6MP Surface Structures on Au(111)[a]

adsorbate		GS (NH_3^+/COO^-/S*/COO^-)		6MP
surface lattice		$(3\sqrt{3} \times \sqrt{3})$R30°		$(3\sqrt{3} \times 2)$
		upright	tilted	
(θ)		0.111	0.111	0.167
E_b/eV		−4.35	−4.97	−2.93
γ/meV·A^{-2}		−64.52	−73.51	−65.18
Bader charge/e	S	−0.10	−0.17	−0.12
	O	-	−1.63	-
	N	-	-	−2.77
	Au	+0.05 (S)	+0.16 (O)	+0.12 (N)
			+0.05 (S)	+0.04 (S)

[a] E_b: binding energy; γ: surface free energy; ⊖: thiol coverage

Even if the "tilted" configuration of adsorbed anionic GSH is energetically more stable, our IR results suggest the presence of a certain amount of GSH molecules in the "upright" zwitterionic form coexisting with "tilted" anionic GSH. This zwitterionic form of GSH, which differs from that in Scheme 1a in the protonation of the carboxylate of the amino acid Gly, yields similar energetic parameters as the anionic "upright" GSH (see Figure S5 and Table S1 in the Supporting Information). In all cases, the shortest distances between S heads of adjacent GSH molecules are 0.5 nm, while the distance between amine and carboxylic acid groups is compatible with the formation of hydrogen bonds, as revealed by PM-IRRA spectra (which could be also formed with adsorbed water molecules that remain on the surface even after drying).

In addition, for the purpose of comparison, DFT calculations have been performed for the protonated form of anionic GSH (which we will term physisorbed GSH; θ = 0.055) and for S adlayers on Au(111) at different coverage (θ = 0.11, 0.17 and 0.33) (see Figure 5 and additional material in the Supporting Information). In the case of S, we have considered θ = 0.11 and 0.17 because they correspond respectively to the coverage of the lattices proposed for GSH and 6MP. It can be seen that, for S coverage >0.11, γ values significantly increase (in absolute value) compared to GS, thus showing that the formation of S adlayers arising from the decomposition of GSH is thermodynamically favored.

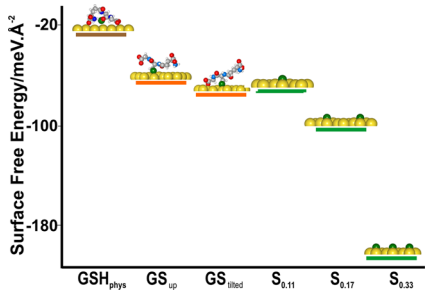

Figure 5. Surface free energies for glutathione species and S monolayers on Au(111). GSH_{phys}: physisorbed GSH (θ = 0.055); GS_{up} and GS_{tilted}: adsorbed GS in the upright or tilted configuration, respectively (θ = 0.11); $S_{0.11}$, $S_{0.17}$ and $S_{0.33}$: S adlayer with θ = 0.11,θ = 0.17 and θ = 0.33, respectively.

GSH/6MP Exchange Experiments on Au(111). As mentioned before, a possible strategy to release biologically relevant thiols (like 6MP) for nanomedicine applications, particularly for drug delivery, is to immobilize them on AuNPs and take advantage of the fact that GSH is found in the cell in millimolar concentrations.[73] In the case of 6MP-capped AuNPs, ligand exchange with 11-mercaptoundecanoic acid and 11-mercapto-1-undecanol has been studied by Pineda et al.[74] The exchange of 6MP (and other thiol-containing drugs) by GSH in AuNPs has been addressed in recent *in vitro* and *in vivo* studies.[18,19] However, in those works the focus was in the drug release process and in the resulting applications rather than on the surface structure and chemistry of the resulting thiol-gold surface. It was therefore interesting to study the thiol exchange on Au(111). Moreover, these studies can help to shed additional light on the stability of GSH molecules on Au(111).

Figure 6 shows a typical CV of the reductive desorption of a 6MP SAM on Au(111) (red line). As already reported, a reductive desorption peak appears at −0.68 ± 0.01 V whose Q value is 54 ± 4 μC cm^{-2} (θ = 0.25).[6,75] Thus, exchange of 6MP by GSH would in principle be feasible due to the difference in peak potentials (E = −0.68 V for 6MP and −0.88 V for GSH).[74] 6MP SAMs on Au(111) were therefore exposed to 5 mM GSH solutions (pH = 7) either for 1, 24, or 48 h, and the resulting SAMs were studied by CV and PM-IRRAS.

After 1 h exposure to GSH solution (Figure 6, gray line) the electroreduction peak E remains at −0.68 ± 0.02 V (as in the blank 6MP CV curve, red line in Figure 6), and Q decreases to 47 ± 7 μC cm^{-2}. Similar results are obtained for 24 h exposure (Figure 6, green line): the peak potential barely changes and Q

DOI: 10.1021/acs.jpcc.5b12643
J. Phys. Chem. C 2016, 120, 14597−14607

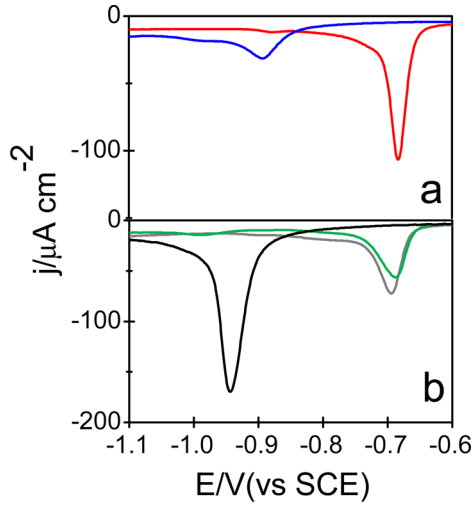

Figure 6. (a) Cyclic voltammograms of 6MP (red line) and GSH (blue line) (t_{SAM} = 1 h; pH = 7) SAMs on Au(111). (b) CVs of 6MP SAMs exposed to 5 mM GSH solution (pH = 7) for different times: 1 h (gray line), 24 h (green line), and 48 h (black line). Scan rate: 0.05 V s^{-1}. Electrolyte: 0.1 M NaOH.

decreases (43 ± 6 μC cm^{-2}). Therefore, while the position of the peak suggests that no significant thiol exchange has occurred, the charge density decrease indicates that a certain amount of the small 6MP molecules are removed when GSH molecules are present, especially for t_{SAM} = 24 h.

Thus, it is reasonable to assume that, in the case of 1 or 24 h exposure of 6MP SAMs to GSH solutions, mixed 6MP/GSH SAMs are formed whose composition, expressed as molar fraction of 6MP (X_{6MP}), is only slightly lower than 1. In order to clarify this point we have prepared mixed GSH/6MP SAMs by competitive adsorption on the clean Au(111) surface from solutions containing different GSH/6MP compositions. To this end, Au(111) substrates were incubated in different 1 mM binary solutions for t_{SAM} = 1 and 24 h. CV results (see Figure S4 in the Supporting Information) show that, as X_{6MP} decreases, E moves slightly in the negative direction and Q decreases, as expected for the higher GSH concentration in solution. However, even for solutions with high GSH concentration (e.g., X_{6MP} = 0.15), the charge density and peak potential of the pure thiol are not attained, in agreement to what has been reported for the case of MBA/undecanethiol mixed SAMs.[76] Also, it is interesting to note that in the case of binary SAMs with t_{SAM} = 24 h desulfurization of GSH is not evident, as there is no clear peak charge increase in comparison to t_{SAM} = 1 h.

We have made additional PM-IRRAS measurements in order to further understand the thiol exchange results shown in Figure 6 for different incubation times. The signature peaks of GSH at ∼1725 and ∼1650 cm^{-1}, which have been assigned to C═O stretching absorptions in free acid and amide, respectively (vide infra), and appear in a region where the 6MP has no absorption peaks, were used to evaluate the presence of GSH on the gold surface upon thiol exchange. On the other hand, the presence of two peaks at ∼1570 and 1590 cm^{-1} (assigned to aromatic ring vibrations; see Table 1) was indicative of the presence of 6MP.[62] Moreover, both molecules (especially 6MP) show strong absorption bands in the 1400 cm^{-1} region.

The PM-IRRA spectrum of a 6MP SAM exposed to 5 mM GSH solution in PB (pH = 7) for 1 h (Figure 7, left, green line) shows bands that match the signature peaks of both 6MP and GSH, as it can be concluded by comparison with 6MP (red line in Figure 7, left) and GSH (blue line) blank spectra. For a 24 h exposure to GSH (Figure 6, center, green line line), the same bands are present. However, the 6MP band at 1590 cm^{-1} is less marked, in agreement with CV data (Figure 6b), which show a slight decrease in the charge of the 6MP desorption peak. The fact that PM-IRRA spectra for 1 and 24 h exposure show characteristic features of both GSH and 6MP are consistent with the formation of 6MP/GSH mixed SAMs mostly composed of 6MP molecules and implies that the release of 6MP induced by GSH on the (111) surface of gold is incomplete at short times. Moreover, the possibility that some GSH molecules may be physisorbed on the remaining 6MP layer, and thus detected by PM-IRRAS, cannot be precluded.

In the case of 6MP SAMs on Au(111) exposed to 5 mM GSH BF pH = 7 for 48 h, cyclic voltammetry (black line in Figure 6b) shows that the peak corresponding to 6MP disappears and a new one appears at E = −0.91 V ± 0.04 V with Q = 88 ± 17 μC cm^{-2}, which can be assigned to the desorption of adsorbed S/polysulfide species. This means that the 6MP SAM is thoroughly removed from the Au(111) surface only when a S adlayer is formed. The Q values are significantly lower than those obtained when 6MP SAMs are exposed to sulfide (H_2S/HS^-) solutions at pH = 7 (see Figure S2b in the Supporting Information), another evidence of the fact that GSH desulfurization is not significant in the incubation solutions.

The corresponding PM-IRRA spectrum (right panel in Figure 7, green line) shows very intense bands characteristic of GSH and the absence of bands characteristic of 6MP like the one at ∼1400 cm^{-1} (those at 1570−1590 cm^{-1} are completely masked by GSH bands). This reveals the presence of physisorbed GSH molecules and/or GSH residues containing

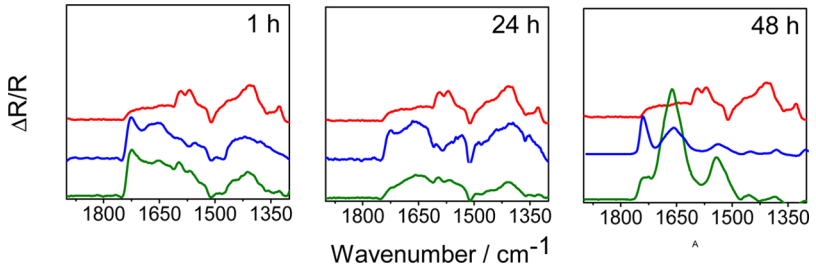

Figure 7. PM-IRRA spectra of 6MP SAMs on Au(111) exposed to 5 mM GSH solutions in phosphate buffer (pH = 7) for different times (green lines). Left: 1 h; center: 24 h; right: 48 h. Related blank spectra for 6MP (red lines) and GSH (blue lines) SAMs are also plotted. The spectra in blue (green) in the right panel have been divided by a factor of 50 (10).

DOI: 10.1021/acs.jpcc.5b12643
J. Phys. Chem. C 2016, 120, 14597−14607

carboxylate groups and amide bonds on the S/polymeric S adlayer. In fact, the spectrum corresponding to the 48 h GSH/6MP exchange is very similar to that of GSH on a S SAM on Au(111) (Figure 3, green line).

In order to gain more insight into the 6MP/GSH exchange results, additional DFT calculations have been performed for 6MP SAMs on Au(111) by employing a $(3\sqrt{3} \times 2)$ unit cell with two 6MP molecules oriented along the [110] direction (θ = 0.17), even if no long-range order is found for these monolayers.[6] Results in Table 2 show that the γ for 6MP and for anionic GSH adsorbed in the upright configuration are very similar (−65.18 vs −64.52 meV Å^{-2}, respectively), while a $(3\sqrt{3} \times \sqrt{3})$R30° lattice of anionic GS species on Au(111) in the tilted configuration yields a more negative value, γ = −73.51 meV Å^{-2}. Moreover, as mentioned before, the γ corresponding to a zwitterionic GSH lattice is comparable to that for anionic GSH in the upright configuration.

The question that now arises is why GSH molecules do not displace a significant amount of the adsorbed 6MP molecules from the Au(111) surface in the exchange experiments. As revealed from γ values, while the $(3\sqrt{3} \times \sqrt{3})$R30° lattice of tilted anionic GS has a higher stability compared to the $(3\sqrt{3} \times 2)$ 6MP lattice, both upright anionic and zwitterionic GS $(3\sqrt{3} \times \sqrt{3})$R30° lattices are similar in stability to the 6MP lattice. In the case of anionic GS, a possible explanation is that the species that arrive at the gold surface cannot attain the most favorable tilted configuration in the presence of a dense, though highly disordered, monolayer of adsorbed 6MP. Indeed, it is possible that, due to sterical hindrance, GSH molecules initially chemisorb in the upright configuration (with similar energetic parameters to 6MP). Eventually, with increasing time (>24 h) more anionic GSH species can attain a tilted configuration and thus induce the removal of some additional 6MP molecules. The adsorbed GSH molecules degrade with time to yield adsorbed S and polysulfide species. In addition, some sulfide species possibly formed by decomposition of the GSH molecules in the vicinity of the Au(111) surface could displace other 6MP molecules due to their strong affinity for this surface, as revealed from DFT calculations. The residues of GSH degradation (and a small amount of intact GSH molecules) adsorb on the S SAM, as revealed by XPS and PM-IRRAS. In summary, the whole process (6MP removal and GSH desulfurization) is rather slow in the presence of a dense 6MP SAM (it takes more than 24 h) because 6MP molecules hinder the approach of GSH to the surface, a requisite for the formation of S species.

The situation is somehow different for the competitive adsorption experiments (see Figure S4 in the Supporting Information), where both species compete for a clean Au(111) surface and GSH/6MP mixed monolayers are formed. In this case more GSH molecules are adsorbed, a fact that can be concluded from the peak shift and the decrease in charge density. Although the adsorption of GSH in the more stable tilted anionic configuration should be energetically favored, the presence of some 6MP molecules on the gold surface and the fact that there are always additional 6MP molecules available from solution are an impediment for the adsorption of a complete GSH monolayer (and for glutathione desulfurization), and thus even at 24 h there are no traces of S species.

CONCLUSIONS

In this paper we have studied GSH SAMs on Au(111) prepared by incubation from neutral phosphate buffer solutions, which has turned out to be a complex system among thiol SAMs on gold. We have found that GSH degrades on Au(111) with increasing immersion time to yield adsorbed S and polysulfide species, a process that is additionally favored by increasing the pH of the incubation solution. The lack of stability of GSH SAMs on the {111} planes of gold at neutral pH has direct relevance for biomedical applications that make use of GSH-capped AuNPs and to understand the physical and chemistry properties of GSH etched nanoclusters. Moreover, it is worth to mention that the presence of the characteristic bands of GSH in the vibrational spectra does not imply that the molecules are adsorbed intact, i.e., without degradation. The stability of GSH was also evaluated in GSH/6MP thiol exchange experiments on Au(111): it was found that a significant displacement of 6MP molecules occurs only for times longer than 24 h and that a S/polysulfide adlayer is formed instead of a GSH SAM. For shorter times, mixed SAMs are formed, a situation that can be accounted for in terms of the surface free energies obtained from DFT calculations. This is of interest for the controlled release of thiol-bearing drugs triggered by GSH when using AuNPs as vehicles. It remains to be determined whether the stability of GSH at physiological pH in other gold planes (e.g., {100}) and/or in surfaces with a high defect density is similar to that of Au(111).

ASSOCIATED CONTENT

Supporting Information

The Supporting Information is available free of charge on the ACS Publications website at DOI: 10.1021/acs.jpcc.5b12643.

Additional cyclic voltammetry experiments for GSH, S, and 6MP/GSH mixed SAMs on Au(111), as well as results from STM imaging of GSH SAMs and DFT calculations of GSH, S, and 6MP SAMs on Au(111) (PDF)

AUTHOR INFORMATION

Corresponding Author

*E-mail: cvericat@inifta.unlp.edu.ar; Phone: +54 221 4257430 ext. 135; Fax: +54 221 4254642.

Author Contributions

The manuscript was written through contributions of all authors. All authors have given approval to the final version of the manuscript.

Notes

The authors declare no competing financial interest.

ACKNOWLEDGMENTS

This work has been financially supported by ANPCyT (PICT 2010-2554 and 2012-0836) and CONICET (PIP 112-200801-00362 and 112-201201-00093), both from Argentina. F.L.M. acknowledges a doctoral fellowship from CONICET. P.C. thankfully acknowledges the computer resources provided by the Computer Support Service for Research (SAII) at La Laguna University. The authors would like to acknowledge Dr. Doris Grumelli for her help with STM analysis.

REFERENCES

(1) Love, J. C.; Estroff, L. A.; Kriebel, J. K.; Nuzzo, R. G.; Whitesides, G. M. Self-Assembled Monolayers of Thiolates on Metals as a Form of Nanotechnology. *Chem. Rev.* **2005**, *105*, 1103−1170.

(2) Vericat, C.; Vela, M. E.; Benitez, G.; Carro, P.; Salvarezza, R. C. Self-Assembled Monolayers of Thiols and Dithiols on Gold: New

DOI: 10.1021/acs.jpcc.5b12643
J. Phys. Chem. C 2016, 120, 14597−14607

Challenges for a Well-Known System. *Chem. Soc. Rev.* **2010**, *39*, 1805−1834.
(3) Kind, M.; Wöll, C. Organic Surfaces Exposed by Self-Assembled Organothiol Monolayers: Preparation, Characterization, and Application. *Prog. Surf. Sci.* **2009**, *84*, 230−278.
(4) Azcárate, J. C.; Corthey, G.; Pensa, E.; Vericat, C.; Fonticelli, M. H.; Salvarezza, R. C.; Carro, P. Understanding the Surface Chemistry of Thiolate-Protected Metallic Nanoparticles. *J. Phys. Chem. Lett.* **2013**, *4*, 3127−3138.
(5) Maksymovych, P.; Voznyy, O.; Dougherty, D. B.; Sorescu, D. C.; Yates, J. T. Gold Adatom as a Key Structural Component in Self-Assembled Monolayers of Organosulfur Molecules on Au (111). *Prog. Surf. Sci.* **2010**, *85*, 206−240.
(6) Pensa, E.; Carro, P.; Rubert, A. A.; Benítez, G.; Vericat, C.; Salvarezza, R. C. Thiol with an Unusual Adsorption-Desorption Behavior: 6-Mercaptopurine on Au(111). *Langmuir* **2010**, *26*, 17068−17074.
(7) Hakkinen, H. The Gold-Sulfur Interface at the Nanoscale. *Nat. Chem.* **2012**, *4*, 443−455.
(8) Bürgi, T. Properties of the Gold-Sulphur Interface: From Self-Assembled Monolayers to Clusters. *Nanoscale* **2015**, *7*, 15553−15567.
(9) Reimers, J. R.; Ford, M. J.; Halder, A.; Ulstrup, J.; Hush, N. S. Gold Surfaces and Nanoparticles Are Protected by Au(0)−Thiyl Species and Are Destroyed When Au(I)−Thiolates Form. *Proc. Natl. Acad. Sci. U. S. A.* **2016**, *113*, E1424−E1433.
(10) Fischer, J. A.; Zoldan, V. C.; Benitez, G.; Rubert, A. A.; Ramirez, E. A.; Carro, P.; Salvarezza, R. C.; Pasa, A. A.; Vela, M. E. Sulfidization of Au(111) from Thioacetic Acid: An Experimental and Theoretical Study. *Langmuir* **2012**, *28*, 15278−15285.
(11) Azcárate, J. C.; Floridia Addato, M. A.; Rubert, A.; Corthey, G.; Kürten Moreno, G. S.; Benítez, G.; Zelaya, E.; Salvarezza, R. C.; Fonticelli, M. H. Surface Chemistry of Thiomalic Acid Adsorption on Planar Gold and Gold Nanoparticles. *Langmuir* **2014**, *30*, 1820−1826.
(12) Maher, P. The Effects of Stress and Aging on Glutathione Metabolism. *Ageing Res. Rev.* **2005**, *4*, 288−314.
(13) Ieva, E.; Trapani, A.; Cioffi, N.; Ditaranto, N.; Monopoli, A.; Sabbatini, L. Analytical Characterization of Chitosan Nanoparticles for Peptide Drug Delivery Applications. *Anal. Bioanal. Chem.* **2009**, *393*, 207−215.
(14) Harfield, J. C.; Batchelor-McAuley, C.; Compton, R. G. Electrochemical Determination of Glutathione: A Review. *Analyst* **2012**, *137*, 2285−2296.
(15) Hostetler, M. J.; Templeton, A. C.; Murray, R. W. Dynamics of Place-Exchange Reactions on Monolayer-Protected Gold Cluster Molecules. *Langmuir* **1999**, *15*, 3782−3789.
(16) Woehrle, G. H.; Brown, L. O.; Hutchison, J. E. Thiol-Functionalized, 1.5-nm Gold Nanoparticles through Ligand Exchange Reactions: Scope and Mechanism of Ligand Exchange. *J. Am. Chem. Soc.* **2005**, *127*, 2172−2183.
(17) Hong, R.; Han, G.; Fernández, J. M.; Kim, B.-j.; Forbes, N. S.; Rotello, V. M. Glutathione-Mediated Delivery and Release Using Monolayer Protected Nanoparticle Carriers. *J. Am. Chem. Soc.* **2006**, *128*, 1078−1079.
(18) Ock, K.; Jeon, W. I.; Ganbold, E. O.; Kim, M.; Park, J.; Seo, J. H.; Cho, K.; Joo, S.-W.; Lee, S. Y. Real-Time Monitoring of Glutathione-Triggered Thiopurine Anticancer Drug Release in Live Cells Investigated by Surface-Enhanced Raman Scattering. *Anal. Chem.* **2012**, *84*, 2172−2178.
(19) Wang, X.; Cai, X.; Hu, J.; Shao, N.; Wang, F.; Zhang, Q.; Xiao, J.; Cheng, Y. Glutathione-Triggered "Off−on" Release of Anticancer Drugs from Dendrimer-Encapsulated Gold Nanoparticles. *J. Am. Chem. Soc.* **2013**, *135*, 9805−9810.
(20) Kumar, D.; Meenan, B.; Dixon, D. Glutathione-Mediated Release of Bodipy® from Peg Cofunctionalized Gold Nanoparticles. *Int. J. Nanomed.* **2012**, *7*, 4007−4022.
(21) Zhang, X.-D.; Luo, Z.; Chen, J.; Song, S.; Yuan, X.; Shen, X.; Wang, H.; Sun, Y.; Gao, K.; Zhang, L.; et al. Ultrasmall Glutathione-Protected Gold Nanoclusters as Next Generation Radiotherapy Sensitizers with High Tumor Uptake and High Renal Clearance. *Sci. Rep.* **2015**, *5*, 8669.
(22) Le Guével, X.; Trouillet, V.; Spies, C.; Jung, G.; Schneider, M. Synthesis of Yellow-Emitting Platinum Nanoclusters by Ligand Etching. *J. Phys. Chem. C* **2012**, *116*, 6047−6051.
(23) Lian, S.; Hu, D.; Zeng, C.; Zhang, P.; Liu, S.; Cai, L. Highly Luminescent near-Infrared-Emitting Gold Nanoclusters with Further Natural Etching: Photoluminescence and Hg^{2+} Detection. *Nanoscale Res. Lett.* **2012**, *7*, 348.
(24) Takehara, K.; Ide, Y.; Aihara, M.; Obuchi, E. An Ion-Gate Response of the Glutathione Monolayer Assembly Formed on a Gold Electrode. *Bioelectrochem. Bioenerg.* **1992**, *29*, 103−111.
(25) Takehara, K.; Aihara, M.; Ueda, N. An Ion-Gate Response of a Glutathione Monolayer Assembly Highly Sensitive to Lanthanide Ions. *Electroanalysis* **1994**, *6*, 1083−1086.
(26) Hepel, M.; Tewksbury, E. Ion-Gating Phenomena of Self-Assembling Glutathione Films on Gold Piezoelectrodes. *J. Electroanal. Chem.* **2003**, *552*, 291−305.
(27) Bieri, M.; Bürgi, T. Adsorption Kinetics of L-Glutathione on Gold and Structural Changes during Self-Assembly: An in situ ATR-IR and QCM Study. *Phys. Chem. Chem. Phys.* **2006**, *8*, 513−520.
(28) Bieri, M.; Bürgi, T. L-Glutathione Chemisorption on Gold and Acid/Base Induced Structural Changes: A PM-IRRAS and Time-Resolved in Situ ATR-IR Spectroscopic Study. *Langmuir* **2005**, *21*, 1354−1363.
(29) Vallée, A.; Humblot, V.; Méthivier, C.; Pradier, C.-M. Glutathione Adsorption from UHV to the Liquid Phase at Various Ph on Gold and Subsequent Modification of Protein Interaction. *Surf. Interface Anal.* **2008**, *40*, 395−399.
(30) Vallée, A.; Humblot, V.; Méthivier, C.; Dumas, P.; Pradier, C.-M. Modifying Protein Adsorption by Layers of Glutathione Pre-Adsorbed on Au(111). *J. Phys.: Condens. Matter* **2011**, *23*, 484002.
(31) Vallée, A.; Humblot, V.; Méthivier, C.; Pradier, C.-M. Adsorption of a Tripeptide, GSH, on Au(111) under UHV Conditions; PM-RAIRS and Low T-XPS Characterisation. *Surf. Sci.* **2008**, *602*, 2256−2263.
(32) Podsiadlo, P.; Sinani, V. A.; Bahng, J. H.; Kam, N. W. S.; Lee, J.; Kotov, N. A. Gold Nanoparticles Enhance the Anti-Leukemia Action of a 6-Mercaptopurine Chemotherapeutic Agent. *Langmuir* **2008**, *24*, 568−574.
(33) Barner, B. J.; Green, M. J.; Saez, E. I.; Corn, R. M. Polarization Modulation Fourier Transform Infrared Reflectance Measurements of Thin Films and Monolayers at Metal Surfaces Utilizing Real-Time Sampling Electronics. *Anal. Chem.* **1991**, *63*, 55−60.
(34) Green, M. J.; Barner, B. J.; Corn, R. M. Real-Time Sampling Electronics for Double Modulation Experiments with Fourier Transform Infrared Spectrometers. *Rev. Sci. Instrum.* **1991**, *62*, 1426−1430.
(35) Frey, B. L.; Corn, R. M.; Weibel, S. C. Polarization-Modulation Approaches to Reflection-Absorption Spectroscopy. In *Handbook of Vibrational Spectroscopy*; John Wiley & Sons: Hoboken, NJ, 2002; Vol. 2.
(36) Kresse, G.; Hafner, J. Ab Initio Molecular Dynamics for Open-Shell Transition Metals. *Phys. Rev. B: Condens. Matter Mater. Phys.* **1993**, *48*, 13115−13118.
(37) Kresse, G.; Furthmüller, J. Efficiency of Ab-Initio Total Energy Calculations for Metals and Semiconductors Using a Plane-Wave Basis Set. *Comput. Mater. Sci.* **1996**, *6*, 15−50.
(38) Dion, M.; Rydberg, H.; Schröder, E.; Langreth, D. C.; Lundqvist, B. I. Van Der Waals Density Functional for General Geometries. *Phys. Rev. Lett.* **2004**, *92*, 246401.
(39) Klimeš, J.; Bowler, D. R.; Michaelides, A. Chemical Accuracy for the van der Waals Density Functional. *J. Phys.: Condens. Matter* **2010**, *22*, 022201.
(40) Blöchl, P. E. Projector Augmented-Wave Method. *Phys. Rev. B: Condens. Matter Mater. Phys.* **1994**, *50*, 17953−17979.
(41) Monkhorst, H. J.; Pack, J. D. Special Points for Brillouin-Zone Integrations. *Phys. Rev. B* **1976**, *13*, 5188−5192.

DOI: 10.1021/acs.jpcc.5b12643
J. Phys. Chem. C 2016, 120, 14597−14607

(42) Dawson, R. M. C.; Elliott, D. C.; Elliott, W. H.; Jones, K. M. *Data for Biochemical Research*, 3rd ed.; Oxford University Press: New York, 1986.
(43) Widrig, C. A.; Chung, C.; Porter, M. D. The Electrochemical Desorption of N-Alkanethiol Monolayers from Polycrystalline Au and Ag Electrodes. *J. Electroanal. Chem. Interfacial Electrochem.* **1991**, *310*, 335−359.
(44) Vericat, C.; Andreasen, G.; Vela, M. E.; Salvarezza, R. C. Dynamics of Potential-Dependent Transformations in Sulfur Adlayers on Au(111) Electrodes. *J. Phys. Chem. B* **2000**, *104*, 302−307.
(45) Baudouin-Cornu, P.; Lagniel, G.; Kumar, C.; Huang, M.-E.; Labarre, J. Glutathione Degradation is a Key Determinant of Glutathione Homeostasis. *J. Biol. Chem.* **2012**, *287*, 4552−4561.
(46) Deshmukh, M.; Kutscher, H.; Stein, S.; Sinko, P. Nonenzymatic, Self-Elimination Degradation Mechanism of Glutathione. *Chem. Biodiversity* **2009**, *6*, 527−539.
(47) Castner, D. G.; Hinds, K.; Grainger, D. W. X-Ray Photoelectron Spectroscopy Sulfur 2p Study of Organic Thiol and Disulfide Binding Interactions with Gold Surfaces. *Langmuir* **1996**, *12*, 5083−5086.
(48) Zhong, C.-J.; Brush, R. C.; Anderegg, J.; Porter, M. D. Organosulfur Monolayers at Gold Surfaces: Reexamination of the Case for Sulfide Adsorption and Implications to the Formation of Monolayers from Thiols and Disulfides. *Langmuir* **1999**, *15*, 518−525.
(49) Gonella, G.; Cavalleri, O.; Terreni, S.; Cvetko, D.; Floreano, L.; Morgante, A.; Canepa, M.; Rolandi, R. High Resolution X-Ray Photoelectron Spectroscopy of 3-Mercaptopropionic Acid Self-Assembled Films. *Surf. Sci.* **2004**, *566−568*, 638−643.
(50) Heister, K.; Zharnikov, M.; Grunze, M.; Johansson, L. S. O. Adsorption of Alkanethiols and Biphenylthiols on Au and Ag Substrates: A High-Resolution X-Ray Photoelectron Spectroscopy Study. *J. Phys. Chem. B* **2001**, *105*, 4058−4061.
(51) Jia, J.; Kara, A.; Pasquali, L.; Bendounan, A.; Sirotti, F.; Esaulov, V. A. On Sulfur Core Level Binding Energies in Thiol Self-Assembly and Alternative Adsorption Sites: An Experimental and Theoretical Study. *J. Chem. Phys.* **2015**, *143*, 104702.
(52) Laiho, T.; Leiro, J. A.; Lukkari, J. XPS Study of Irradiation Damage and Different Metal−Sulfur Bonds in Dodecanethiol Monolayers on Gold and Platinum Surfaces. *Appl. Surf. Sci.* **2003**, *212−213*, 525−529.
(53) Vericat, C.; Vela, M. E.; Andreasen, G.; Salvarezza, R. C.; Vázquez, L.; Martín-Gago, J. A. Sulfur−Substrate Interactions in Spontaneously Formed Sulfur Adlayers on Au(111). *Langmuir* **2001**, *17*, 4919−4924.
(54) Lustemberg, P. G.; Vericat, C.; Benitez, G. A.; Vela, M. E.; Tognalli, N.; Fainstein, A.; Martiarena, M. L.; Salvarezza, R. C. Spontaneously Formed Sulfur Adlayers on Gold in Electrolyte Solutions: Adsorbed Sulfur or Gold Sulfide? *J. Phys. Chem. C* **2008**, *112*, 11394−11402.
(55) Calborean, A.; Martin, F.; Marconi, D.; Turcu, R.; Kacso, I. E.; Buimaga-Iarinca, L.; Graur, F.; Turcu, I. Adsorption Mechanisms of L-Glutathione on Au and Controlled Nano-Patterning through Dip Pen Nanolithography. *Mater. Sci. Eng., C* **2015**, *57*, 171−180.
(56) Nuzzo, R. G.; Dubois, L. H.; Allara, D. L. Fundamental Studies of Microscopic Wetting on Organic Surfaces. 1. Formation and Structural Characterization of a Self-Consistent Series of Polyfunctional Organic Monolayers. *J. Am. Chem. Soc.* **1990**, *112*, 558−569.
(57) Lin-Vien, D.; Colthup, N. B.; Fateley, W. G.; Grasselli, J. G. *The Handbook of Infrared and Raman Characteristic Frequencies of Organic Molecules*; Academic Press: San Diego, CA, 1991.
(58) Kisailus, D.; Truong, Q.; Amemiya, Y.; Weaver, J. C.; Morse, D. E. Self-Assembled Bifunctional Surface Mimics an Enzymatic and Templating Protein for the Synthesis of a Metal Oxide Semiconductor. *Proc. Natl. Acad. Sci. U. S. A.* **2006**, *103*, 5652−5657.
(59) Fears, K. P.; Creager, S. E.; Latour, R. A. Determination of the Surface Pk of Carboxylic- and Amine-Terminated Alkanethiols Using Surface Plasmon Resonance Spectroscopy. *Langmuir* **2008**, *24*, 837−843.
(60) Jordon, C. E.; Frey, B. L.; Kornguth, S.; Corn, R. M. Characterization of Poly-L-Lysine Adsorption onto Alkanethiol-Modified Gold Surfaces with Polarization-Modulation Fourier Transform Infrared Spectroscopy and Surface Plasmon Resonance Measurements. *Langmuir* **1994**, *10*, 3642−3648.
(61) Lawrie, G.; Keen, I.; Drew, B.; Chandler-Temple, A.; Rintoul, L.; Fredericks, P.; Grøndahl, L. Interactions between Alginate and Chitosan Biopolymers Characterized Using FTIR and XPS. *Biomacromolecules* **2007**, *8*, 2533−2541.
(62) Bu, Y.; Huan, S.; Liu, X.; Shen, G.; Yu, R. Multiple-Angle-of-Incidence Polarization Infrared Reflection-Absorption Spectroscopy (MAI-PIRRAS) for Investigation of 6-Mercaptopurine SAMs on Smooth Silver Surface. *Vib. Spectrosc.* **2009**, *49*, 38−42.
(63) Wieland, T. Chemistry and Properties of Glutathione. In *Glutathione: Proceedings of the Symposium Held at Ridgefield, Connecticut, November, 1953*; Colowick, S., Schwarz, D. R., Lazarow, A., Eds.; Academic Press: New York, 1954.
(64) Danehy, J. P. The Alkaline Decomposition of Aliphatic Disulfides. In *The Chemistry of Organic Sulfur Compounds*; Kharasch, N., Meyers, C. Y., Eds.; Pergamon Press: London, 1966; pp 337−349.
(65) Routh, J. I. The Decomposition of Cysteine in Aqueous Solution. *J. Biol. Chem.* **1939**, *130*, 297−304.
(66) Aruga, M.; Awazu, S.; Hanano, M. Kinetic Studies on Decomposition of Glutathione. III. Peptide Bond Cleavage and Desulfurization in Aqueous Solution. *Chem. Pharm. Bull.* **1980**, *28*, 521−528.
(67) Robbins, F. M.; Fioriti, J. A. Alkaline Degradation of Cystine, Glutathione and Sulphur-Containing Proteins. *Nature* **1963**, *200*, 577−578.
(68) Asquith, R. S.; Carthew, P. The Preparation and Subsequent Identification of a Dehydroalanyl Peptide from Alkali-Treated Oxidised Glutathione. *Biochim. Biophys. Acta, Protein Struct.* **1972**, *285*, 346−351.
(69) Jones, A. J.; Helmerhorst, E.; Stokes, G. B. The Formation of Dehydroalanine Residues in Alkali-Treated Insulin and Oxidized Glutathione. A Nuclear-Magnetic-Resonance Study. *Biochem. J.* **1983**, *211*, 499−502.
(70) Meister, A.; Tate, S. S. Glutathione and Related Γ-Glutamyl Compounds: Biosynthesis and Utilization. *Annu. Rev. Biochem.* **1976**, *45*, 559−604.
(71) Ballatori, N.; Krance, S. M.; Notenboom, S.; Shi, S.; Tieu, K.; Hammond, C. L. Glutathione Dysregulation and the Etiology and Progression of Human Diseases. *Biol. Chem.* **2009**, *390*, 191−214.
(72) Ramírez, E. A.; Cortés, E.; Rubert, A. A.; Carro, P.; Benítez, G.; Vela, M. E.; Salvarezza, R. C. Complex Surface Chemistry of 4-Mercaptopyridine Self-Assembled Monolayers on Au(111). *Langmuir* **2012**, *28*, 6839−6847.
(73) Chompoosor, A.; Han, G.; Rotello, V. M. Charge Dependence of Ligand Release and Monolayer Stability of Gold Nanoparticles by Biogenic Thiols. *Bioconjugate Chem.* **2008**, *19*, 1342−1345.
(74) Reyes, E.; Madueño, R.; Blázquez, M.; Pineda, T. Facile Exchange of Ligands on the 6-Mercaptopurine-Monolayer Protected Gold Clusters Surface. *J. Phys. Chem. C* **2010**, *114*, 15955−15962.
(75) Madueño, R.; Pineda, T.; Sevilla, J. M.; Blázquez, M. An Electrochemical Study of the Sams of 6-Mercaptopurine (6MP) at Hg and Au(111) Electrodes in Alkaline Media. *Langmuir* **2002**, *18*, 3903−3909.
(76) González, M. C. R.; Orive, A. G.; Carro, P.; Salvarezza, R. C.; Creus, A. H. Structure and Electronic and Charge-Transfer Properties of Mercaptobenzoic Acid and Mercaptobenzoic Acid−Undecanethiol Mixed Monolayers on Au(111). *J. Phys. Chem. C* **2014**, *118*, 30013−30022.

DOI: 10.1021/acs.jpcc.5b12643
J. Phys. Chem. C 2016, 120, 14597−14607